Trans. of the Society of Instrument and Control Engineers
Vol.E-3, No.1, 91/97 (2004)

Adaptive Estimation of Component Proportion in a Pixel of a Multispectral Image

Senya KIYASU* and Sadao FUJIMURA**

Spectral unmixing is a method by which to estimate the proportion of each component in a pixel using multispectral data. In conventional analysis of remotely sensed images, each pixel is classified into a single object category. However, the actual land surface corresponding to a pixel does not necessarily consist of only one category of object. Therefore, estimating the proportion of components that exist in a pixel is often useful. The most commonly used method of spectral unmixing assumes that the component spectra are determined from training data. However, available training data do not always correctly represent the spectral characteristics of the categories within the objective area. In such cases, large errors may appear in the results of unmixing.

We herein propose the adaptive spectral unmixing method, which estimates suitable component spectra from the actual observed data and thus requires no training data. By adaptively estimating the component spectra from the set of observed data in the objective area, we can correctly estimate the proportion of components even if the spectral characteristics change with the location of objective area. In the proposed method, the spectral reflectance of pixels is expressed by vectors in multi-dimensional space, which can be written as linear combinations of component spectra weighted according to component proportion. We determine the component spectra by finding the minimum volume of simplex containing all of the reflectance vectors, where the vertices of the simplex correspond to the component spectra.

We estimated the degree of errors by numerical simulation and compared the performance of the proposed adaptive method to that of the conventional method. We confirmed that the proposed method of adaptive unmixing provides better results than the conventional method when the spectral characteristics change with the location of the objective area.

Key Words: remote sensing, spectral unmixing, spectral reflectance, training data, representativeness

1. Introduction

In remote sensing, objects on the land surface are recognized based on multi-spectral images acquired by aircraft or earth observation satellites. In many cases, the images are classified, and each pixel is assigned to a single category based on the spectral characteristics of objects.

When pixels are classified, we assume that the land surface area that corresponds to a pixel is covered by only one category of object. However, when a pixel corresponds to a large area on the land surface, several categories of objects often exist within the pixel. In such cases, we cannot determine the specific category for a small fraction of the pixel. Moreover, mixed pixels often demonstrate intermediate spectral characteristics of component spectra and may be misclassified as not belonging to any of the component categories.

On the other hand, spectral unmixing is a method in which more than one category is assigned to a pixel and the proportion of each component that exists in the pixel is estimated [1). Usual methods of spectral unmixing are based on the linear mixing model, which assumes that the component spectra are added linearly to compose the observed spectra [1)~3)]. However, this method often exhibits large errors when applied to actual observed data. The main reasons for these large errors may be that the 1) mixing process of real objects cannot be assumed to be linear, and 2) the component spectra used to estimate the proportions of the components are not suitable for unmixing. In the present paper, we focus on the latter of the above problems.

In the conventional method of spectral unmixing, we estimate the component spectra using the provided training data for each category and estimate the proportion in a pixel. However, if the provided training data do not correctly represent the objective category, the estimated spectra will not agree with the spectral characteristics in the pixel, and the result of unmixing will not be accurate [2)]. This problem of a lack of representativeness in training data causes both unmixing error and misclassi-

* Graduate School of Engineering, The University of Tokyo, Bunkyo-ku, Tokyo, Japan
(currently at Nagasaki University)
** Graduate School of Engineering, The University of Tokyo, Bunkyo-ku, Tokyo, Japan
(currently at Teikyo Heisei University)

fication[4]. In the present paper, we propose a method of adaptively estimating the component spectra from observed data in order to solve the problem of representativeness in training data.

Several methods for estimating the component spectra from observed mixture spectra have been investigated. One such method was first studied by Lawton and Sylvester[5], and a criteria of entropy was introduced by Sasaki et al.[6]. However, these methods do not provide correct results when applied directly to the remotely sensed images, because few of the component objects in remote sensing have specific peaks in the spectra.

In recent studies on remote sensing, methods have been proposed for spectral unmixing without known component spectra[7),8)]. However, neither the influence of insufficient representativeness of training data nor the effectiveness of adaptive estimation has been clarified. In the present paper, we focus on the fact that insufficient representativeness of training data is one of the essential reasons for error of unmixing and propose a method to solve this problem. We propose a method for adaptively estimating the component spectra from observed data and demonstrate the effectiveness of the proposed method.

2. Spectral Unmixing for Multispectral Image

First, we describe the problem of ordinary methods of spectral unmixing, which estimates component spectra from training data.

2.1 Spectral unmixing based on linear mixing model

Ordinary methods of spectral unmixing are based on the linear mixing model. Let us assume that there are N categories of objects that exist in the image, which is composed of M pixels. When a multispectral image is observed at L wavelengths, where $\lambda_1, \cdots, \lambda_L$, the observed spectrum of the i-th pixel is expressed as $\boldsymbol{x}_i = (x_{i1}, \cdots, x_{iL})^t$ for $i = 1, \cdots, M$, where t denotes the transpose of a matrix.

When the mixing process of a spectrum can be expressed as a linear combination of component spectra weighted according to component proportion, the observed vector $\boldsymbol{x}_i$ can be written as linear combinations of $\boldsymbol{s}_j$ as

$$\boldsymbol{x}_i = c_{i1}\boldsymbol{s}_1 + c_{i2}\boldsymbol{s}_2 + \cdots + c_{iN}\boldsymbol{s}_N, \tag{1}$$

where $\boldsymbol{s}_j = (s_{j1}, \cdots, s_{jL})^t$ for $j = 1, \cdots, N$ are the component spectra, and c_{ij} are the proportions of component j in pixel i. We can write this relation in matrix form as

$$\boldsymbol{x}_i = \boldsymbol{S}\,\boldsymbol{c}_i, \tag{2}$$

where $\boldsymbol{S}$ is a matrix in which the columns are component spectra $\boldsymbol{s}_j$, and $\boldsymbol{c}_i = (c_{i1}, \cdots, c_{iN})^t$ is a proportion vector. The proportion of each component corresponds to the amount of area that the category of object occupies in a pixel. Therefore, the proportion vectors $\boldsymbol{c}_i$ are constrained by the following relations:

$$\sum_{j=1}^{N} c_{ij} = 1, \tag{3}$$

$$c_{ij} \geq 0. \tag{4}$$

Spectral unmixing is a processing of determining $\boldsymbol{c}_i$ for given $\boldsymbol{x}_i$ by using the component spectra $\boldsymbol{S}$. The conventional method assumes that the component spectra $\boldsymbol{S}$ are known. If the vectors $\boldsymbol{s}_j$ are linearly independent, then the proportion of each component $\boldsymbol{c}_i$ can be determined using the generalized inverse matrix as [1),2)]

$$\boldsymbol{c}_i = (\boldsymbol{S}^t\boldsymbol{S})^{-1}\,\boldsymbol{S}^t\,\boldsymbol{x}_i. \tag{5}$$

When we use actual observed data, the estimated component proportion vector $\boldsymbol{c}_i$ often does not satisfy constraints (3) and (4). In such cases, we should determine the proportion vectors $\boldsymbol{c}_i$ such that the difference between the observed vector $\boldsymbol{x}_i$ and its estimation $\boldsymbol{S}\,\boldsymbol{c}_i$ is minimized. Therefore, we estimate the component proportion by taking the vector $\boldsymbol{c}_i$, which satisfies the following condition:

$$|\,\boldsymbol{x}_i - \boldsymbol{S}\,\boldsymbol{c}_i\,| \longrightarrow \min \tag{6}$$

under restrictions (3) and (4) [1),2)].

2.2 Problems in the estimation of component spectra using training data

In order to estimate the component spectra using the above method, we must know the component spectra $\boldsymbol{S}$ beforehand. In actual applications, the component vectors $\boldsymbol{s}_j$ are usually derived from a set of training samples that are extracted from known areas in the image. However, the component vectors do not always correctly agree with the spectral characteristics of the components within the object area. There are several possible reasons for this[2]. For example, the training data may not correctly represent the object categories. Moreover, the spectral characteristics may have large variation, even within the same category. Furthermore, the observed spectral data may have been affected by large measurement errors. Therefore, if the spectral characteristics of the training area differ from those of the objective area, they may cause large errors in the results of the estimation of component proportion.

3. Adaptive Estimation of Component Proportion in a Pixel

When the spectral characteristics change with the location of the objective area, we must use appropriate component spectra for the objective area in order to accurately estimate the component proportion. However, it is almost impossible to obtain the necessary training data for each of the different objective areas. Therefore, we attempt to adaptively estimate the component spectra from observed data and use them to estimate the component proportion.

Our purpose is to estimate the component vectors $\boldsymbol{s}_j$ from observed vectors $\boldsymbol{x}_i$ in a image that contain several categories of unknown proportion in each pixel. After the component vectors $\boldsymbol{s}_j$ have been determined, the component proportion vector $\boldsymbol{c}_i$ should be estimated by a conventional method according to equation (5) or equation (6).

3.1 Principle of estimation of component spectra

An observed vector is expressed as a linear combination of N component vectors, as shown in equation (1). Since the results should always satisfy the constraints of equations (3) and (4), all of the observed vectors $\boldsymbol{x}_i$ that can be considered as points in a multidimensional space should exist inside of the $N-1$ dimensional simplex, the vertices of which are defined by the component vectors $\boldsymbol{s}_1, \cdots, \boldsymbol{s}_N$. If a pixel consists of one category of object, the observed vector corresponds to one of the vertices of the simplex and is equal to a component spectrum. However, since we do not know where the pure pixel exists in the image, the component spectra are unknown. We estimate the component spectra by finding the vertices of simplex in the multidimensional space, as shown in **Fig. 1**.

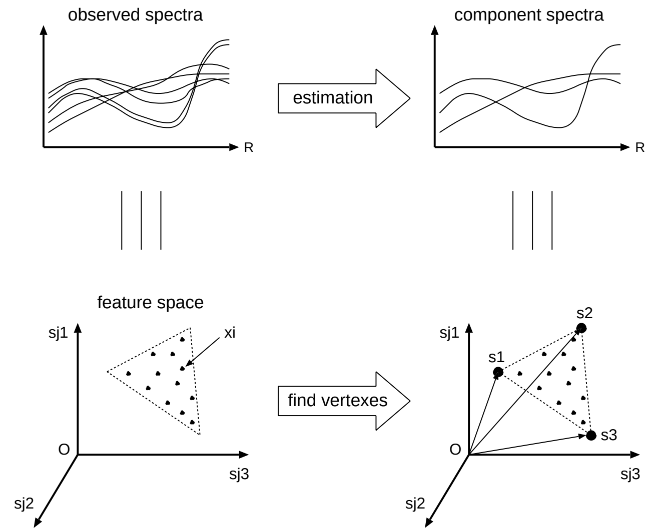

Fig. 1 Estimation of component spectra by finding the vertexes in multidimensional space

Let us assume an N–1-dimensional simplex X_0, the vertices of which correspond to component vectors. When the vertices $\boldsymbol{a}_1, \cdots, \boldsymbol{a}_N$ are given, we can calculate the volume of the simplex as follows [9]:

$$\frac{1}{(N-1)\,!}\ \mathrm{abs}\left|\begin{array}{cccc} 1 & 1 & \cdots & 1 \\ \boldsymbol{a}_1 & \boldsymbol{a}_2 & \cdots & \boldsymbol{a}_N \end{array}\right|, \tag{7}$$

where "abs $|\cdot|$" refers to the absolute value of the determinant. We denote the volume of the simplex X_0 as Q_0. Each observed vector will exist inside the simplex X_0, and pure pixels correspond to the vertices of X_0.

Next, we consider any $N-1$-dimensional simplex X that includes all of the observed vectors inside of it. When we express the volume of the simples X as Q, the relationship $Q \geq Q_0$ always holds. Then, Q will take the minimum value ($= Q_0$) when the simplex X is equal to the simplex X_0, where the vertices of the simplex correspond to the component vectors.

Therefore, we can estimate the unknown component vectors by finding the minimum volume of the simplex that includes all of the observed vectors.

3.2 Algorithm of estimation [10]

We estimate the component vectors by a non-linear optimization technique. Although the dimension of the observed vectors becomes large as the number of bands increases, the observed vectors can still be expressed in an N-dimensional space, which is defined by the component vectors $\boldsymbol{s}_1, \cdots, \boldsymbol{s}_N$. Therefore, we derive N basis vectors from the observed vectors and express all of the observed vectors in the feature space spanned by the basis vectors. Using this method, we can also process several hundred dimensional hyperspectral data in the same sequence.

When the number of components is N, we express the component spectra $\boldsymbol{s}_j$ as a linear combination of orthonormal basis vectors $\boldsymbol{v}_1, \cdots, \boldsymbol{v}_N$, as follows:

$$\boldsymbol{s}_j = t_{j1}\boldsymbol{v}_1 + t_{j2}\boldsymbol{v}_2 + \cdots + t_{jN}\boldsymbol{v}_N, \tag{8}$$

where t_{jk} are coefficients of basis vectors. We calculate the second moment matrix as

$$\boldsymbol{R} = \sum_{i=1}^{M} \boldsymbol{x}_i\,\boldsymbol{x}_i^t \,/\, M \tag{9}$$

and use its eigenvectors as the basis vectors [6], where M is the number of observed vectors. The eigenvectors span a feature space in which the component spectrum $\boldsymbol{s}_j$ and the observed vector $\boldsymbol{x}_i$ are represented by the points

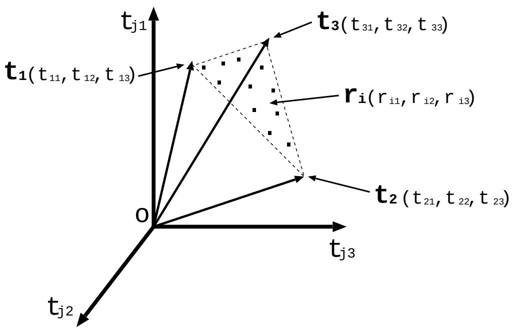

Fig. 2 Observed vector and component vector expressed in a feature space

$\boldsymbol{t}_j = (t_{j1}, \cdots, t_{jN})^t$ and $\boldsymbol{r}_i = (r_{i1}, \cdots, r_{iN})^t$, respectively, where

$$\boldsymbol{t}_j = \boldsymbol{V}^t \boldsymbol{s}_j, \tag{10}$$

$$\boldsymbol{r}_i = \boldsymbol{V}^t \boldsymbol{x}_i, \tag{11}$$

and $\boldsymbol{V} = (\boldsymbol{v}_1, \cdots, \boldsymbol{v}_N)$.

From equations (2), (10), and (11), we obtain

$$\boldsymbol{r}_i = \boldsymbol{V}^t \boldsymbol{S} \boldsymbol{c}_i = \boldsymbol{T} \boldsymbol{c}_i, \tag{12}$$

where $\boldsymbol{T} = (\boldsymbol{t}_1, \cdots, \boldsymbol{t}_N)$. This means that we can express the vector $\boldsymbol{r}_i$ as a linear combination of $\boldsymbol{t}_1, \cdots, \boldsymbol{t}_N$ as

$$\boldsymbol{r}_i = c_{i1}\boldsymbol{t}_1 + c_{i2}\boldsymbol{t}_2 + \cdots + c_{iN}\boldsymbol{t}_N. \tag{13}$$

Since the coefficients c_{ij} are restricted by equations (3) and (4), $\boldsymbol{r}_i$ exists inside of the $N-1$-dimensional simplex defined by $\boldsymbol{t}_1, \cdots, \boldsymbol{t}_N$. In the case in which the number of categories is three, the inside of the triangle shown in **Fig. 2** corresponds to the existing region of the observed vectors.

Next, we find the minimum volume of simplex, which includes all of the points $\boldsymbol{r}_i$. We define an object function U and find the vectors $\boldsymbol{t}_1, \cdots, \boldsymbol{t}_N$ that minimize the function U. The object function is defined as

$$U = Q + P \longrightarrow \min, \tag{14}$$

were Q is the volume of the N–1-dimensional simplex and P is the penalty function that expresses the nonnegative constraints of the component spectrum and the proportion. We used the penalty function P as [6]:

$$P = \gamma \{ \sum_{j=1}^{N} \sum_{l=1}^{L} F(s_{jl}) + \sum_{i=1}^{M} \sum_{j=1}^{N} F(c_{ij}) \}, \tag{15}$$

where γ is a scaling factor and $F(\cdot)$ is the function of

$$F(x) = \begin{cases} 0 & \text{if } x \geq 0 \\ x^2 & \text{if } x < 0. \end{cases} \tag{16}$$

After the vectors $\boldsymbol{t}_j$ are determined, component spectra $\boldsymbol{s}_j$ can be calculated by equation (8).

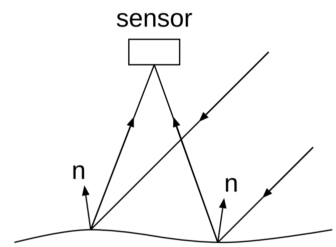

Fig. 3 Angles of incidence and reflection, which change with viewing angle

4. Consideration of Accuracy by Numerical Simulation [11]

We assumed the situation in which the spectral characteristics change with the location of the objective area and considered the estimation error of component proportion. We used a simple model of reflectance variation [2] and evaluated the accuracy of the proposed method by numerical simulation.

Since the reflectance of objects usually changes with the incident and reflected angles, the reflectance will change with the viewing angle of the sensor, as shown in **Fig. 3**. In such cases, training data that have been acquired from a specific region in the image may not accurately represent the characteristics throughout the entire image. We assume different variation ratios r_i for different categories i and introduce the variation model as [2]

$$\boldsymbol{s}_{oi} = (1 + r_i)\, \boldsymbol{s}_i. \tag{17}$$

The spectral reflectances of five objects (four types of plant leaves and stone) measured by a spectrometer [12] were used as component spectra. The spectral range was from 510 to 750 nm, and the number of spectral bands was 49. We generated the observed spectra by linear combinations of various proportion of components and added a normally distributed level of random noise, the standard deviation of which was set to 0.5% of the reflectance. We evaluated the cases in which the numbers of categories are three, four, and five, respectively, and compared the results of estimation. We compared the accuracies of component proportion obtained by the conventional method to that obtained by the proposed method.

For three categories, **Fig. 4** shows the 31 observed spectra generated from the assumed components: stone, fallen leaves, and young leaves. The estimated vertices in the feature space are shown in **Fig. 5**, where the observed spectra are included within the triangle. We used the "simplex method" for numerical processing of nonlinear optimization. The scale parameter of the penalty function

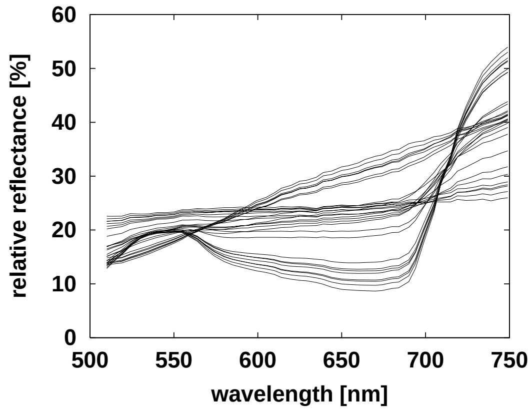

Fig. 4 Observed spectra

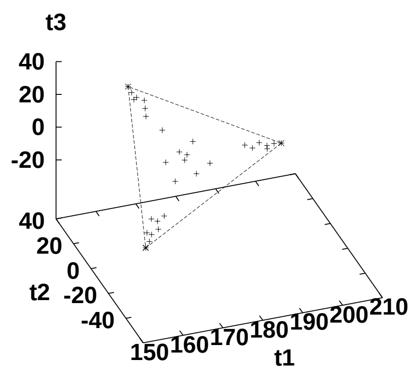

Fig. 5 Estimation of component spectra in a feature space

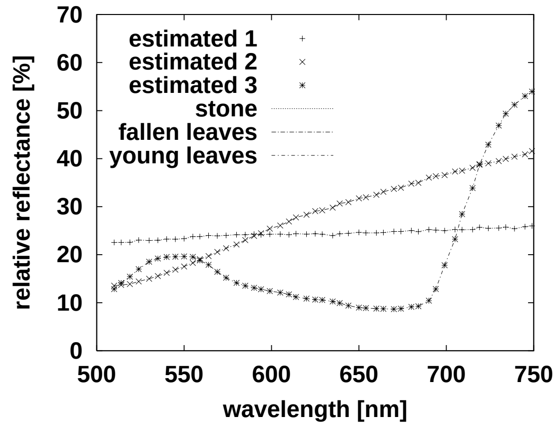

Fig. 6 Estimated component spectra and true spectra

Table 1 Results of conventional estimation and adaptive estimation when the number of categories is three

variation of reflectance			method of estimation	category [%] stone	fallen	young
a	stone: 0% fallen: 1% young: 2%	1	(true value)	33.0	33.0	34.0
			conventional	31.3	34.9	33.8
			adaptive	32.8	33.2	33.9
		2	(true value)	25.0	25.0	50.0
			conventional	22.6	27.2	50.1
			adaptive	24.8	25.0	50.2
b	stone: 1% fallen: 2% young: 4%	1	(true value)	33.0	33.0	34.0
			conventional	29.3	37.3	33.4
			adaptive	32.8	33.2	33.9
		2	(true value)	25.0	25.0	50.0
			conventional	20.3	29.8	49.9
			adaptive	24.8	25.0	50.2
c	stone: 3% fallen: 5% young: 7%	1	(true value)	33.0	33.0	34.0
			conventional	25.4	42.3	32.2
			adaptive	32.8	33.2	33.9
		2	(true value)	25.0	25.0	50.0
			conventional	16.2	34.7	49.2
			adaptive	24.8	25.0	50.2

was set to $\gamma = 1$ for the first iteration and was multiplied by ten for each iteration until $\gamma = 10^{10}$.

The estimated component spectra and the assumed true spectra agreed well, as shown in **Fig. 6**. An example of estimated component proportion is shown in **Table 1**. The reflectances of objects changed in the three different patterns, and the proportion of components were estimated for two cases: (stone, fallen, young) = (33%, 33%, 34%) and (25%, 25%, 50%). The error of estimation was reduced when the component spectra were adaptively estimated and used. On the other hand, there were errors of up to 10% when the conventional method was used.

The relationships between the true and estimated proportions for various types of component ratios are shown in **Fig. 7**. The estimated value obtained by the conventional method has large errors, as shown in Fig. 7(a). On the other hand, most of the estimated results obtained by proposed estimation were positioned along the diagonal line, as shown in Fig. 7(b), which indicates that the estimated value agrees well with the true value. Thus, the proposed method of adaptive estimation of component spectra enables accurate estimation of the component proportion in a pixel without the influence of the variation of the spectral characteristics in an image.

Table 2 shows the result of estimation when the number of categories is four and 37 spectral data were generated and used. The relationship between the true value and the estimated value is shown in **Fig. 8**. The result for five categories and 45 observed spectra is shown in **Fig. 9**.

Although the error of estimation increased with the number of categories, the proposed method always gives better results than the conventional method. In the present experiment, we obtained stable results when the number of categories N was up to five. However, the process of optimization will become difficult for large N,

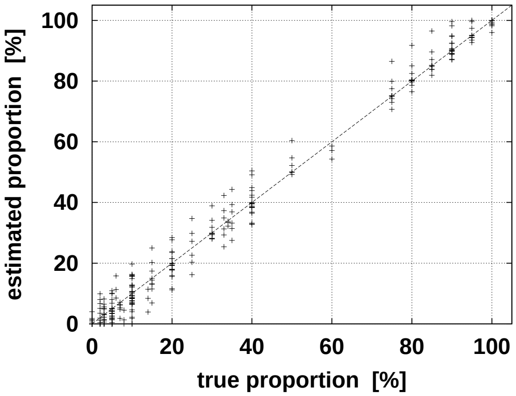

(a) conventional estimation

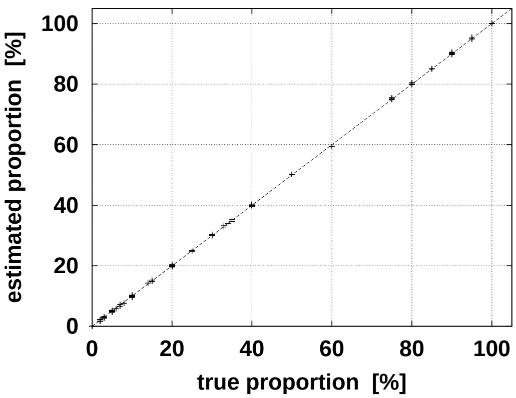

(b) adaptive estimation

Fig. 7 Correspondence of the true value and the estimated value of component proportion when the number of categories is three

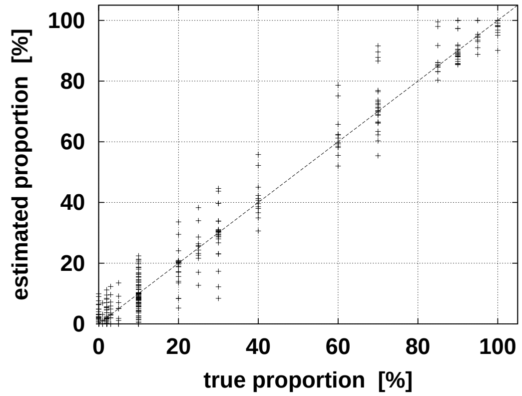

(a) conventional estimation

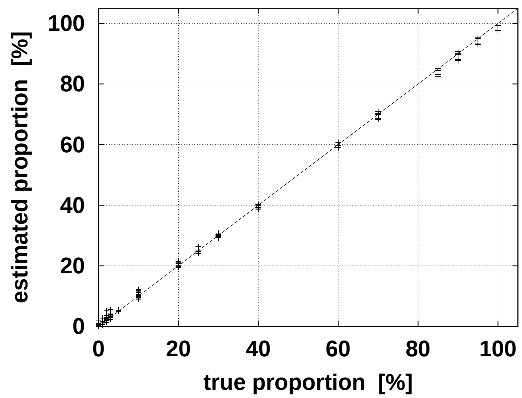

(b) adaptive estimation

Fig. 8 Correspondence of the true value and the estimated value of component proportion when the number of categories is four

Table 2 Results of conventional estimation and adaptive estimation when the number of categories is four

variation of reflectance		method of estimation		category [%] stone	fallen	young	yellow
	[%]		(true value)	40.0	30.0	20.0	10.0
	stone: 0	1	conventional	38.0	29.9	20.2	11.9
a	fallen: 1		adaptive	39.8	30.0	19.6	10.3
	young: 2		(true value)	25.0	25.0	25.0	25.0
	yellow: 3	2	conventional	21.6	24.3	25.5	28.6
			adaptive	26.4	25.2	24.7	24.1
			(true value)	40.0	30.0	20.0	10.0
	stone: 1	1	conventional	34.9	29.2	20.5	15.4
b	fallen: 2		adaptive	39.8	30.1	19.6	10.3
	young: 4		(true value)	25.0	25.0	25.0	25.0
	yellow: 8	2	conventional	17.0	23.2	25.8	34.0
			adaptive	26.4	25.2	24.7	24.1
			(true value)	40.0	30.0	20.0	10.0
	stone: 3	1	conventional	30.6	28.7	20.9	19.8
c	fallen: 5		adaptive	39.8	30.0	19.6	10.3
	young: 7		(true value)	25.0	25.0	25.0	25.0
	yellow: 9	2	conventional	12.7	22.6	26.4	38.3
			adaptive	26.4	25.2	24.7	24.1

because a total of N^2 parameters must be optimized.

5. Conclusions

We have proposed a method of spectral unmixing that accurately estimates the proportion of components in a pixel. This method does not use training data and adaptively estimates the component spectra from observed data and uses them for unmixing. We have shown that the components in mixed pixels can be accurately estimated when the spectral characteristics change with the location of objective area. The results of numerical simulation show that the accuracy of estimation is improved in cases where insufficient representativeness of training data causes large errors when using the conventional method. The application of this method to a remotely sensed actual observed image and the estimation of the number of categories from observed data are problems for future study.

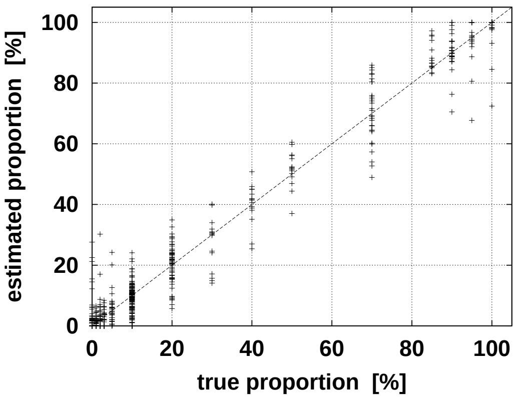

(a) conventional estimation

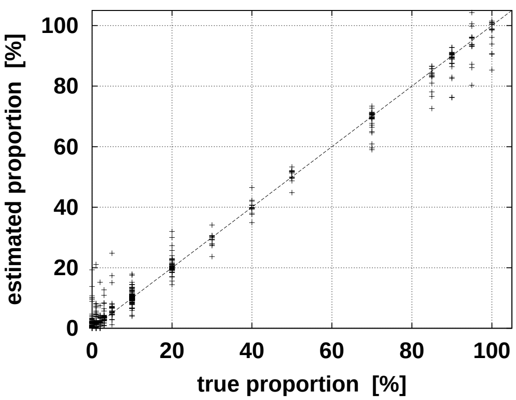

(b) adaptive estimation

Fig. 9 Correspondence of the true value and the estimated value of the component proportion when the number of categories is five

References

1) M. Inamura: Analysis of Remotely Sensed Image Data by means of Category Decomposition, Trans. IEICE, **J-70-C**-2, 241/250 (1987)
2) T. Ito, S. Fujimura: Estimation of Cover Area of Each Category in a Pixel by Pixel Decomposition into Categories, Trans. SICE, **23**-8, 800/805 (1987)
3) J.J. Settle and N.A. Drake: Linear mixing and the estimation of ground cover proportions, Int. J. Remote Sensing, **14**-6, 1159/1177 (1993)
4) S. Fujimura, H. Toyota, T. Aikoh, Y. Suzuki: Comparison of Automatic Classification Methods for Multispectral Images, Trans. SICE, **14**-3, 269/276 (1978)
5) W.H. Lawton and E.A. Sylvester: Self Modeling Curve Resolution, Technometrics, **13**-3, 617/633 (1971)
6) K. Sasaki, S. Kawata and S. Minami: Estimation of Component Spectral Curves from Unknown Mixture Spectra, Applied Optics, **23**-12, 1955/1959 (1984)
7) J.W. Boardman and F.A. Kruse: Automated spectral analysis: A geologic example using AVIRIS data, north Grapevine Mountains, Nevada, Proc. Tenth Thematic Conference on Geologic Remote Sensing, Environmental Research Institute of Michigan, I407/I418 (1994)
8) W. Rosenthal: Estimating Alpine Snow Cover With Unsupervised Spectral Unmixing, IEEE Proc. IGARSS'96, 2252/2254 (1996)
9) Mathematical Society of Japan (Ed.): Encyclopedia of Mathematics (3rd Ed.), Iwanami Shoten (1985)
10) S. Kiyasu, S. Fujimura: Adaptive Estimation of Component Spectra from Multispectral Images, J. of Teikyo Heisei Univ., **13**-1, 33/38 (2001)
11) S. Kiyasu, S. Fujimura: Adaptive Estimation of Component Proportion in a Pixel Considering Variation of Spectral Reflectance, Proc. 39th SICE Annual Conference, 301-A-2(CD-ROM) (2000)
12) S. Fujimura, I. Satoh, K. Ban, N. Yamada, M. Ishikawa: Imaging Spectrometer with High Sensitivity and High Resolution, Proc. 51st JSAP Annual Meeting, 52 (1990)

Senya Kiyasu (Member)

He received a B.S. degree in mathematical engineering and information physics from the University of Tokyo in 1986. From 1986 to 1991, he worked at the Production Engineering Research Laboratory of Hitachi Ltd. He was a research associate at the University of Tokyo from 1991 to 2000. From 2000 to 2003, he worked at Teikyo Heisei University as a lecturer. Since 2003 he has been a associate professor at Nagasaki University. His research interests are in pattern information processing, pattern recognition and remote sensing.

Sadao Fujimura (Member)

He received the B. Sc., M. Sc., and Dr. Eng. degrees in applied physics from the University of Tokyo, Tokyo, Japan in 1963, 1965 and 1968, respectively. He is currently a Professor of the Department of Information Science, Teikyo Heisei University. He served as a lecturer for the Department of Mathematical Engineering and Information Physics, the University of Tokyo from 1968 to 1973. He joined the University of Electro-Communications, Tokyo, as an associate professor, and in 1978 rejoined the Department above of the University of Tokyo as an associate professor. He became a professor in 1988, and retired in 2000, and is a professor emeritus of the University of Tokyo. From 1980 to 1981 he was a visiting professor at the Department of Electric Engineering, University of Tennessee, Knoxville, Tennessee. His research interests are in image processing, pattern recognition, infrared thermometry, remote sensing and 3D distribution and shape measurement. He is a fellow of the Society of Instrument and Control Engineers, a senior member of IEEE, a member of the Japan Society of Applied Physics, and so forth.

Reprinted from Trans. of the SICE
Vol. 39 No. 2 97/103 2003